

See discussions, stats, and author profiles for this publication at: <https://www.researchgate.net/publication/321234294>

Modeling Insight into Battery Electrolyte Electrochemical Stability and Interfacial Structure

Article in *Accounts of Chemical Research* · November 2017

DOI: 10.1021/acs.accounts.7b00486

CITATIONS

0

READS

90

6 authors, including:



Oleg Borodin

Army Research Laboratory

215 PUBLICATIONS 5,884 CITATIONS

[SEE PROFILE](#)



Jenel Vatamanu

University of Utah

49 PUBLICATIONS 1,402 CITATIONS

[SEE PROFILE](#)



Kang Xu

Army Research Laboratory

212 PUBLICATIONS 8,611 CITATIONS

[SEE PROFILE](#)

Some of the authors of this publication are also working on these related projects:



Poly(propylene oxide) structure and dynamics [View project](#)



NMC materials [View project](#)

All content following this page was uploaded by [Kang Xu](#) on 24 November 2017.

The user has requested enhancement of the downloaded file.

Modeling Insight into Battery Electrolyte Electrochemical Stability and Interfacial Structure

Published as part of the *Accounts of Chemical Research* special issue “Energy Storage: Complexities Among Materials and Interfaces at Multiple Length Scales”.

Oleg Borodin,^{*,†} Xiaoming Ren,[†] Jenel Vatamanu,[†] Arthur von Wald Cresce,[†] Jaroslaw Knap,[‡] and Kang Xu[†]

[†]Electrochemistry Branch, Sensors and Electron Devices Directorate, US Army Research Laboratory, 2800 Powder Mill Rd., Adelphi, Maryland 20783, United States

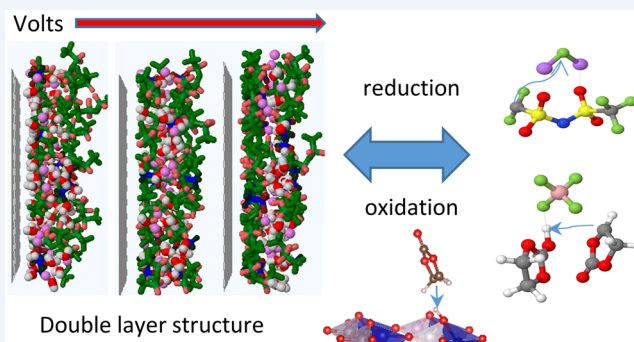
[‡]Simulation Sciences Branch, RDRL-CIH-C, US Army Research Laboratory, Aberdeen Proving Ground, Maryland 21005-5066, United States

Supporting Information

CONSPECTUS: Electroactive interfaces distinguish electrochemistry from chemistry and enable electrochemical energy devices like batteries, fuel cells, and electric double layer capacitors. In batteries, electrolytes should be either thermodynamically stable at the electrode interfaces or kinetically stable by forming an electronically insulating but ionically conducting interphase. In addition to a traditional optimization of electrolytes by adding cosolvents and sacrificial additives to preferentially reduce or oxidize at the electrode surfaces, knowledge of the local electrolyte composition and structure within the double layer as a function of voltage constitutes the basis of manipulating an interphase and expanding the operating windows of electrochemical devices. In this work, we focus on

how the molecular-scale insight into the solvent and ion partitioning in the electrolyte double layer as a function of applied potential could predict changes in electrolyte stability and its initial oxidation and reduction reactions. In molecular dynamics (MD) simulations, highly concentrated lithium aqueous and nonaqueous electrolytes were found to exclude the solvent molecules from directly interacting with the positive electrode surface, which provides an additional mechanism for extending the electrolyte oxidation stability in addition to the well-established simple elimination of “free” solvent at high salt concentrations. We demonstrate that depending on their chemical structures, the anions could be designed to preferentially adsorb or desorb from the positive electrode with increasing electrode potential. This provides additional leverage to dictate the order of anion oxidation and to effectively select a sacrificial anion for decomposition. The opposite electroadsorption behaviors of bis(trifluoromethane)sulfonimide (TFSI) and trifluoromethanesulfonate (OTF) as predicted by MD simulation in highly concentrated aqueous electrolytes were confirmed by surface enhanced infrared spectroscopy.

The proton transfer (H-transfer) reactions between solvent molecules on the cathode surface coupled with solvent oxidation were found to be ubiquitous for common Li-ion electrolyte components and dependent on the local molecular environment. Quantum chemistry (QC) calculations on the representative clusters showed that the majority of solvents such as carbonates, phosphates, sulfones, and ethers have significantly lower oxidation potential when oxidation is coupled with H-transfer, while without H-transfer their oxidation potentials reside well beyond battery operating potentials. Thus, screening of the solvent oxidation limits without considering H-transfer reactions is unlikely to be relevant, except for solvents containing unsaturated functionalities (such as C=C) that oxidize without H-transfer. On the anode, the F-transfer reaction and LiF formation during anion and fluorinated solvent reduction could be enhanced or diminished depending on salt and solvent partitioning in the double layer, again giving an additional tool to manipulate the order of reductive decompositions and interphase chemistry. Combined with experimental efforts, modeling results highlight the promise of interphasial compositional control by either bringing the desired components closer to the electrode surface to facilitate redox reaction or expelling them so that they are kinetically shielded from the potential of the electrode.



INTRODUCTION

Lithium ion batteries (LIBs) dominate energy storage for portable electronics and are penetrating automotive and grid-storage

Received: September 30, 2017

applications. Further progress depends not only on the development of new high capacity electrode, but also on tailoring electrolytes in order to support fast and yet reversible lithium transport through the bulk electrolyte and across interfaces. Electrolytes must be either thermodynamically stable with electrodes or form a stable passivation layer that should be electronically insulating but ionically conducting while accommodating mechanical stresses due to electrode volume changes during battery cycling. The passivation layer on the anode is called the solid electrolyte interphase (SEI) to highlight its electrolyte nature while being an independent material phase with multiple components. The passivation layer on the cathode is often called the cathode electrolyte interphase (CEI) to distinguish it from SEI, but its existence is sometimes controversial and depends on cathode chemistries. Electrolyte stability with electrodes has been recognized as the key property dictating the success of next generation battery chemistries.

The commonly used LIB electrolyte consists of a mixture of linear and cyclic carbonates as solvents along with numerous functional additives and cosolvents, examples of which include unsaturated esters, nitriles, and phosphates. Cyclic carbonates such as ethylene carbonate (EC) remain indispensable components and are usually responsible for salt dissociation and SEI formation, while linear carbonates such as dimethyl carbonate (DMC) typically acts as diluents to render solutions less viscous and more conductive at lower temperatures.^{1,2} Most electrolyte solvents and salt anions, with the exception of lithium halides and Li₂O, are not thermodynamically stable at potentials where lithium metal deposits or Li⁺ inserts into graphite or silicon. These solvents and anions decompose, forming lithium alkyl-carbonates or carbonates in the outer SEI, and LiF and Li₂O in the inner SEI on graphite, lithium, or Si.^{1,3–5} In order to understand which electrolyte component dominates the interphase chemistry, it is vitally important to know the relative reduction and oxidation potentials of each electrolyte component, as those with the highest reduction potential would contribute most to the initial components of SEI. Note that redox potential of an electrolyte component is dependent on its local environment. Control of the preferential reduction via salt concentration or other factors enables novel SEI.⁶ Interestingly, electrolyte reduction may also occur at low voltage cathodes such as sulfur and result in a beneficial CEI that could dramatically prevent cathode dissolution and capacity fade.⁷

To calculate oxidation and reduction stability of the representative complexes versus Li/Li⁺, the energy cycle shown in Figure 1 is used. Equation 1 relates the absolute oxidation potential of a complex M relative to an electron at rest in vacuum, ($E_{\text{abs}}^{\circ}(\text{M})$) using the cycle shown in Figure 1a.

$$E_{\text{abs}}^{\circ}(\text{M}) = [\Delta G_{\text{e}} + \Delta G_{\text{S}}^{\circ}(\text{M}^{+}) - \Delta G_{\text{S}}^{\circ}(\text{M})]/F \quad (1)$$

where ΔG_{e} is the ionization free energy in gas-phase at 298.15 K. Two types of ionization potentials are considered: vertical and adiabatic. For the vertical oxidation, the complex geometry does not change during electron transfer, while optimized or relaxed geometry is used during calculation of the adiabatic oxidation. $\Delta G_{\text{S}}^{\circ}(\text{M}^{+})$ and $\Delta G_{\text{S}}^{\circ}(\text{M})$ are the free energies of solvation of the oxidized and initial complexes, M⁺ and M, respectively, and F is the Faraday constant. $E_{\text{abs}}^{\circ}(\text{M})$ is related to the Li/Li⁺ scale by subtracting 1.4 V as discussed elsewhere.^{8,9} Note, the solvent variation is expected to change this factor by 0.1–0.3 V because of the variation of the lithium free energy of solvation.⁸

We focus on understanding of the key electrochemical oxidation and reduction reactions. The first question we address is

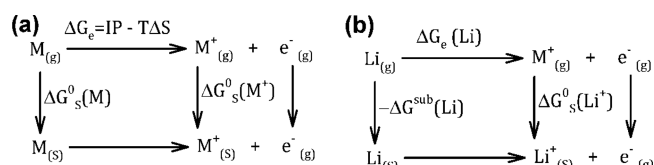


Figure 1. Free-energy cycle for the redox reaction ($\text{M} \rightarrow \text{M}^{+} + \text{e}^{-}$), where $\text{M}_{(\text{g})}$ denotes molecule M in gas-phase, $\text{M}_{(\text{s})}$ denotes the solvated molecule, and IP denotes ionization potential.

the size of the representative model systems that is required to accurately capture them in quantum chemistry (QC) calculations. To understand the influence of salt concentration and electrolyte composition on electrochemical stability, we combine the representative QC calculations on small model electrolyte clusters and density functional theory (DFT) studies of solvent reactions on the cathode surfaces with insight obtained from larger-scale molecular dynamics (MD) simulations of bulk and interfacial electrolyte properties at electrode surfaces.

OXIDATION STABILITY OF SIMPLIFIED ELECTROLYTE MODELS

The most widely considered descriptors for electrolyte stability are the highest occupied molecular orbital (HOMO) and lowest unoccupied molecular orbital (LUMO) of the isolated solvent molecules and vertical redox stability. They are obtained from the most computationally expedient QC calculations that do not include geometry optimization of the reduced or oxidized complexes. A test of 100 carbonate and 300 phosphate molecules, however, showed that the difference between vertical and adiabatic oxidation potential could be as high as 1.8 V indicating that molecular geometry relaxation during oxidation is important.¹⁰ An even more profound influence of relaxation was found on the reduction potentials.¹⁰ Thus, we conclude that while computationally expedient HOMO, LUMO, and vertical oxidation and reduction stability calculations often correlate well with experimental data, large deviations could be observed. Survey of the oxidation and reduction potentials calculated using DFT for isolated molecules indicated an excellent correlation for redox shuttle molecules^{11,12} with maximum deviations as little as 0.15–0.25 eV but significant deviations for main electrolyte solvents and anions.^{8,13,14}

In order to understand the reasons behind the failure of QC calculations on isolated molecules surrounded by an implicit solvent like the polarized continuum to predict oxidation stability, we add the second solvent or anion explicitly in QC calculations as shown in Figure 2 for EC/PF₆⁻, 1,2-dimethoxyethane (DME)/TFSI, and a vinylene carbonate (VC) additive. Intrinsic oxidation potentials for the isolated EC solvent molecules surrounded by implicit solvent with $\epsilon = 20$ was around 6.9 V vs Li/Li⁺, making it clear that direct oxidation of EC does not occur during battery operations. During oxidation of the EC/PF₆⁻ complex, HF formation occurs lowering the oxidation potential. H-transfer to another EC coupled with oxidation decreased oxidation potential further to 5–5.2 V, which is almost 2 V lower than the oxidation potential of isolated EC. The coupling of H-transfer with carbonate oxidation has been confirmed by electron paramagnetic resonance.¹⁵ Oxidation of the VC(PF₆⁻) complex also happens around 5 V, but it did not require any H-transfer and minimal molecular deformations as evidenced by small $E_{\text{vert}} - E_{\text{ad}}$. Experimentally, a significantly higher (by 10²–10³ times) oxidation current is observed when

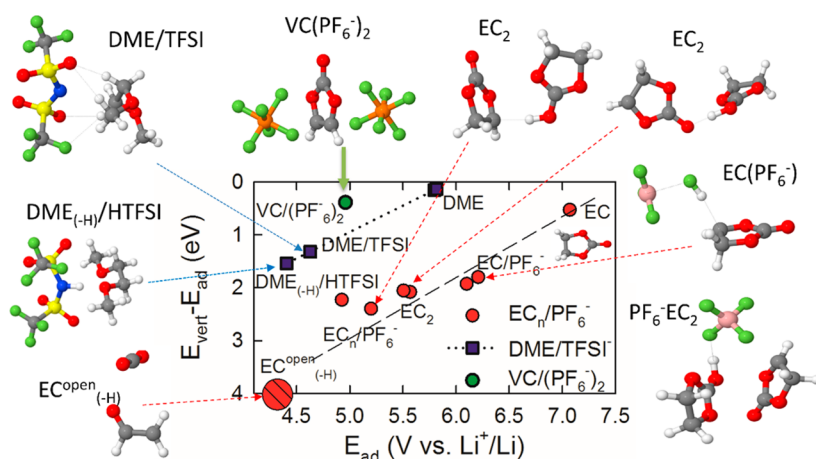


Figure 2. Oxidation potentials of solvates from QC calculations using G4MP2 for the $\text{EC}_n/\text{PF}_6^-$ and DME/TFSI^- complexes⁵⁷ and M05-2X/6-31+G(d,p) for $\text{VC}/(\text{PF}_6^-)_2$ with SMD ($\epsilon = 20$) implicit solvent model. The difference between vertical (E_{vert}) and adiabatic (E_{ad}) oxidation potentials is from the M05-2X/6-31+G(d,p) calculations.

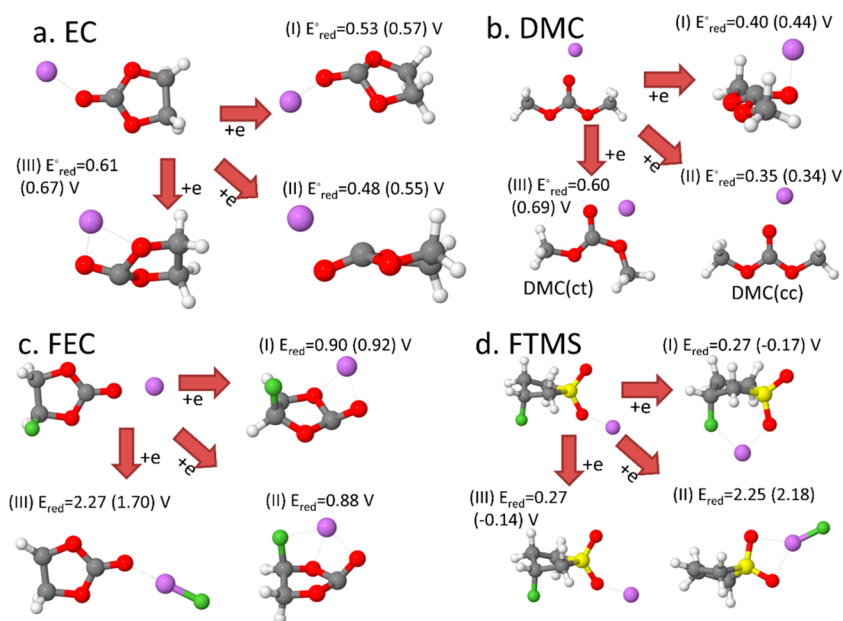


Figure 3. Optimized geometries of the neutral and reduced Li^+ -solvent complexes I-III from QC calculations. Reduction potentials of EC (a), DMC (b), FEC (c), and 2-fluorotetramethylene sulfone (FTMS) (d) are given vs Li/Li^+ from G4MP2 QC calculations using SMD ($\epsilon = 20$) implicit solvent model.^{10,58} Values in parentheses are from LC- ω PBE/6-31 + G(d,p) (a,b) and M05-2X/6-31+G(d,p) (c,d) DFT calculations.

VC is added to the EC-based electrolyte around 5 V,^{8,16} consistent with QC predictions. The difference between E_{vert} and E_{ad} oxidation potentials is suggested as a marker associated with the reorganization energy that is used to estimate reaction kinetics. Thus, plotting oxidation potentials versus ($E_{\text{vert}} - E_{\text{ad}}$) allows us to include kinetics into electrolyte screening and relate QC calculations performed on representative clusters to the linear sweep voltammetry (LSV) experiments that yield the rate of oxidation reaction versus potential. One has to keep in mind that due to the finite rate of LSV scans, experiments tend to yield an oxidation potential higher than the thermodynamic oxidation potential.¹⁷ Because the slow oxidation processes occurring at the lowest potentials are often the most relevant to the long-term stability of electrolytes in batteries, we suggest that the smallest complexes used in QC screening should include at least H-donor and H-acceptor molecules.

H-transfer reactions during oxidation are not limited to carbonates. They occur for DME/TFSI^- as shown in Figure 2. The presence of TFSI^- near DME stabilizes the hole after the electron transfer resulting in a lower oxidation potential. H-transfer from DME to nitrogen of TFSI^- leads to even lower oxidation potentials but is expected to be slower than the DME/TFSI^- oxidation without H-transfer due to the additional reorganization energy required for H-transfer. Alkyl phosphates and sulfones also have significantly lower oxidation potentials after H-transfer indicating that it occurs for the majority of electrolyte solvents with the exception of compounds with unsaturated functionalities such as VC.^{8,16} A good correlation is observed between the trend shown in Figure 2 and the LSV experiments.^{9,16}

The above oxidation scenarios are particularly relevant for nonactive electrodes such as glassy carbon or conductive

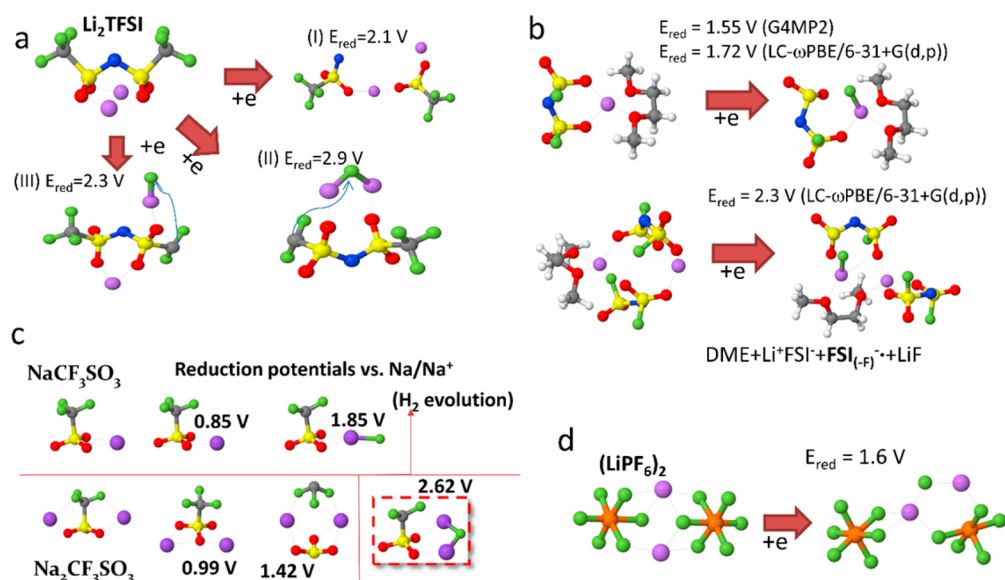


Figure 4. Optimized geometries and reduction potentials vs Li/Li^+ obtained from QC calculations at the G4MP2 level unless specified otherwise.^{7,16,32,34}

additives that have few H-accepting groups on the surface. Active transition metal oxide and phosphate cathodes, on the other hand, possess plentiful under-coordinated oxygen atoms available at surfaces for the solvent dehydrogenation reaction. DFT calculations showed that EC undergoes H-transfer and surface hydroxylation on fully charged high-voltage $\text{Ni}_{0.5}\text{Mn}_{1.5}\text{O}_4$ spinel (111) and (001) surfaces,¹⁰ $\text{Li}_x\text{Mn}_2\text{O}_4$ spinel (111) surfaces,¹⁸ and layered oxide-based cathodes.¹⁹ At increasing cathode state of charge, the reaction barrier and reaction energy become more favorable to this dehydrogenation/hydroxylation reaction pair. Giordano et al.¹⁹ concluded that H-transfer from EC to the cathode surface of layered oxides was found to be energetically more favorable than nucleophilic attack, electrophilic attack, and EC dissociation with oxygen extraction from the oxide surface. The propensity of such H-transfer reactions coupled with the reduction of the interfacial transition metal ions with lowered Fermi level relative to the O 2p band center is associated with less lithium content or replacement of cobalt by nickel.¹⁹ Because alkyl phosphates, sulfones, and ethers were shown to undergo H-transfer coupled with oxidation in bulk solvents as linear and cyclic carbonates do,⁸ we suggest that these compounds behave similarly to EC and undergo dehydrogenation on high voltage cathode surface. Thus, development of electrolyte additives should be centered around surface deactivation or polymerization reactions followed by H-transfer from solvents,²⁰ for example, preferential H-transfer coupled with oxidation followed by polymerization of tris(trimethylsilyl) phosphate (TMSP) compared to mixed carbonate electrolytes.¹⁶ Polymer formation would diminish H-transfer reactions lowering the $-\text{OH}$ surface concentration, which was recently shown to initiate transition metal dissolution by weakening M–O bonds.²¹

■ PREDICTION OF REDUCTION STABILITY FROM QUANTUM CHEMISTRY

Understanding electrolyte reduction in multicomponent electrolytes is critical for optimizing the SEI. Two factors largely determine the order in which electrolyte components reduce and decompose: (a) the intrinsic reduction potential of the

$(\text{Li}^+)_n(\text{solvent})$ or $(\text{Li}^+)_n(\text{anion})$ complex and (b) the ability of the solvent or anion to complex the Li^+ in order to stabilize the transferred electron. Reduction potentials are obtained from simple QC calculations for the $\text{Li}^+(\text{EC})$, $\text{Li}^+(\text{DMC})$, $\text{Li}^+(\text{FEC})$, and $\text{Li}^+(\text{FTMS})$ are shown in Figure 3. Electron transfer to the $\text{Li}^+(\text{EC})$ complex (Figure 3a) yields at least three stable complexes that are at minima as confirmed by frequency analysis. The reduction potentials of these complexes are within 0.2 eV, contributing to a broadening of the reduction peaks in the CV measurements. Different reduction geometries are expected to yield different barriers for reductive decomposition, yet most studies focused on the $\text{Li}^+(\text{EC}^\bullet)$ ring opening starting only from one initial configuration (I) in Figure 3a.²² QC studies of the decomposition pathways, including competition between one- and two-electron reduction, have been reviewed elsewhere.^{3,22–25} The $\text{Li}^+(\text{DMC})$ complex also has multiple stable reduction complexes. Complex I is the most stable for the DMC(cis–cis) conformer. It is 0.2 eV less stable, however, than complex III, which is the most stable for the DMC(cis–trans) conformer. Comparison of EC/ Li^+ and DMC(cis–cis)/ Li^+ reduction potentials indicates a preferential reduction for EC versus DMC when DMC(cis–cis) is a dominant conformer.

The $\text{Li}^+(\text{fluoroethylene carbonate, FEC})$ complex also has multiple reduction products as noted by Leung.²⁶ Reduction potentials for complexes I and II are slightly higher than the value of 0.75 V reported from MP2 calculations by Leung,²⁶ and are in good agreement with the experimental value of 0.95 V.²⁷ Complex III results in LiF formation occurring during reduction yielding a much higher reduction potential. Because of the large reorganization energy for this reaction and lower Li^+ binding energy to fluorine compared to carbonyl oxygen by 0.3 eV, the reduction pathway III is expected to be slower than reduction pathways I and II.¹⁰ These predictions are consistent with experiments.²⁸ Note that LUMO screening predicts much smaller increases in electrolyte reduction with fluorination because it misses LiF-forming pathways.^{10,29} Partially fluorinated sulfone electrolytes also undergo LiF formation (see Figure 3d) if the $\text{Li}\cdots\text{F}$ contacts are feasible. Adding second and

third solvent explicitly did not significantly change predicted reduction potentials as shown in SI of ref 30.

LiF formation during salt reduction also increases reduction potential, as shown in Figure 4, providing that contact ion pairs and aggregates form with $\text{Li}\cdots\text{F}$ contacts as was observed only at high salt concentrations.³¹ The $(\text{Li}^+)_2\text{TFSI}^-$ reduction potential varies significantly from 2.1 V vs Li/Li^+ depending on the reaction from N–S bond breaking at 2.1 V to Li_2F formation as high as 2.9 V. All these reactions occur at potentials significantly higher than the reduction of the isolated TFSI^- predicted to be around 1.4 V vs Li/Li^+ . High reduction potential for $(\text{Li}^+)_2\text{TFSI}$ aggregates formed in a highly concentrated $\text{LiTFSI}-\text{H}_2\text{O}$ is partially responsible for the LiF-rich SEI formation in aqueous electrolytes and the subsequent extension of the electrochemical stability window.³² LiF and NaF also increased the reduction potential of other salts giving an additional control parameter for preferential LiF and NaF formation and anion decomposition at anodes or cathodes and tailoring SEI or CEI formation.^{33,34}

LITHIUM COORDINATION ENVIRONMENT

Understanding and accurate prediction of the Li^+ solvation shell composition is important for tailoring the solvent and anion reduction order and the Li^+ desolvation processes.^{16,30,35–37}

Typically, calculations of the Li^+ (solvent) binding energies in gas phase were used in order to understand composition of the lithium solvation shell. Figure 5 shows the gas-phase binding energies of $\text{Li}^+(\text{EC})$ and $\text{Li}^+(\text{DMC})$ from QC calculations. The $\text{DMCcc}-\text{Li}^+$ complex is much less stable than the $\text{DMCct}-\text{Li}^+$ complex due to a smaller dipole moment of the former. Interestingly, Li^+ binding to both of the noncarbonyl

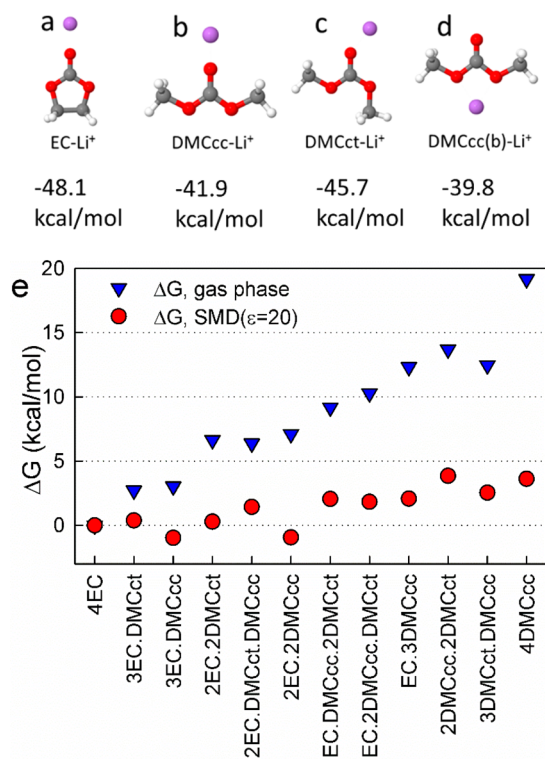


Figure 5. Binding energy for EC and DMC to the Li^+ cation from G4 QC calculations in gas phase (a–d).⁴² The relative cluster binding energies from PBE/6-31+G(d,p) calculations with SMD ($\epsilon = 20$) and in gas-phase for $(\text{EC})_n(\text{DMC})_m-\text{Li}^+$, $n + m = 4$. ΔE and ΔG refer to relative energies and free energies, respectively (e).⁴²

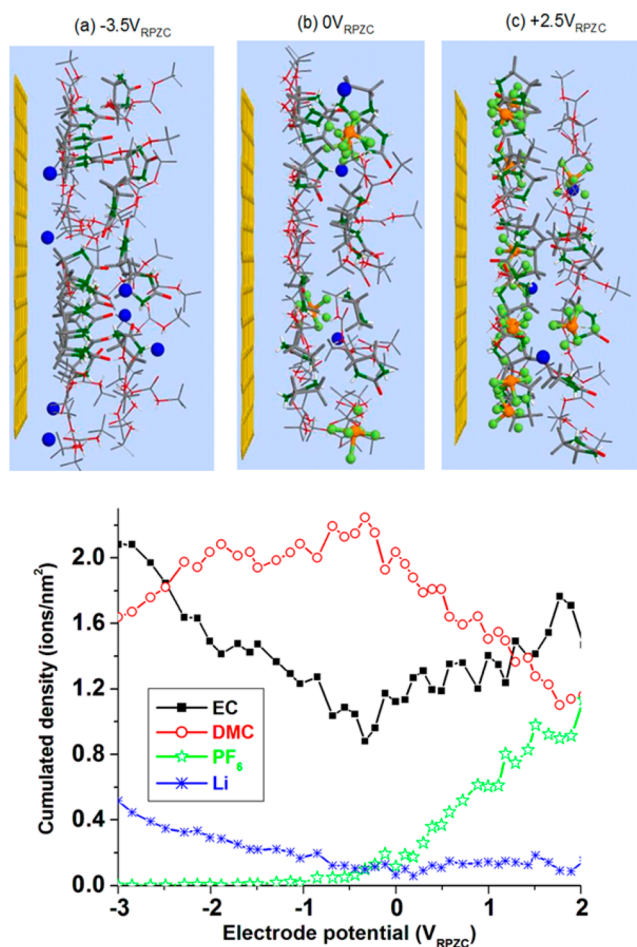


Figure 6. Snapshots from MD simulations⁴⁴ of EC/DMC(3:7) 1 M LiPF_6 at three voltages, interfacial density of electrolyte components. Adapted with permission from ref 44. Copyright 2012 American Chemical Society.

ether-like oxygens of DMCcc (denoted as $\text{DMCcc}(b)-\text{Li}^+$) is only $2.2 \text{ kcal mol}^{-1}$ less stable than the $\text{DMCcc}-\text{Li}^+$ complex where Li^+ is bound to carbonyl oxygen. Based upon these binding energies, the Li^+ first solvation shell is expected to be dominated by EC with a few percent of DMCct and an even smaller contribution from DMCcc in contradiction to Raman³⁸ and infrared³⁹ (IR) spectroscopy studies but in a reasonable agreement with NMR interpretation.^{40,41} The explicit inclusion of four solvents changes the relative EC versus DMC contributions as shown in Figure 5e. In the four solvent-coordinated Li^+ solvates in gas-phase, substitution of EC with DMCcc was more energetically favorable than with DMCct . Inclusion of an implicit solvent beyond the Li^+ first solvation shell further stabilized the four solvent-containing solvates containing DMCcc . The $(\text{EC})_3(\text{DMCcc})-\text{Li}^+$ and $(\text{EC})_2(\text{DMCcc})_2-\text{Li}^+$ solvates become the most stable, even more stable than $(\text{EC})_4-\text{Li}^+$. This stabilization is largely due to a smaller dipole–dipole repulsion between the relatively nonpolar DMCcc with EC. When Boltzmann factors are used to estimate of the population of EC and DMC in the Li^+ solvation shell, a ratio of 1.9 to 1 is obtained in good agreement with BOMD simulations⁴² that explicitly considered all solvent and reanalyzed Raman and IR spectra using DFT-based activity and intensity changes upon Li^+ complexation.⁴²

Further examination of Figure 5e shows that in the EC-rich regime the DMCcc conformer is preferred to DMCct , while

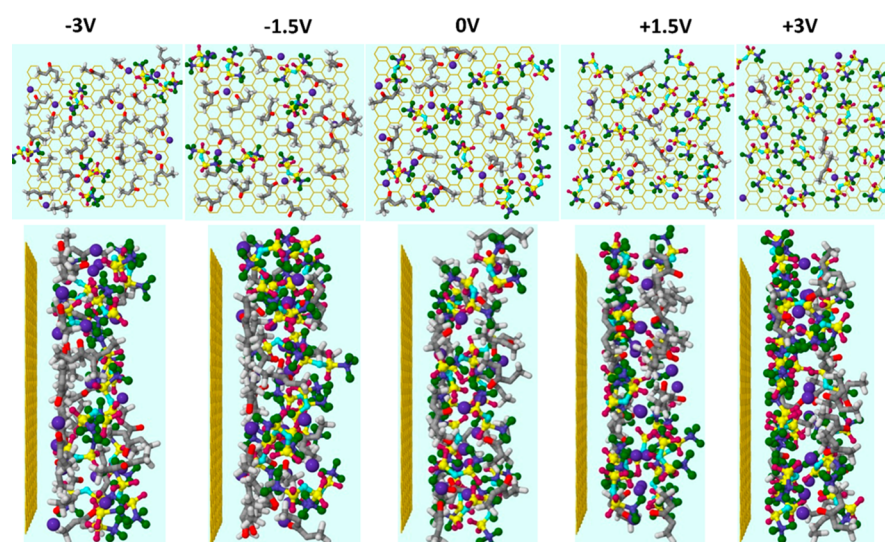


Figure 7. Snapshots on the interfacial structure from MD simulations of $(\text{DMC})_{12}\text{LiTFSI}$ at 363 K.

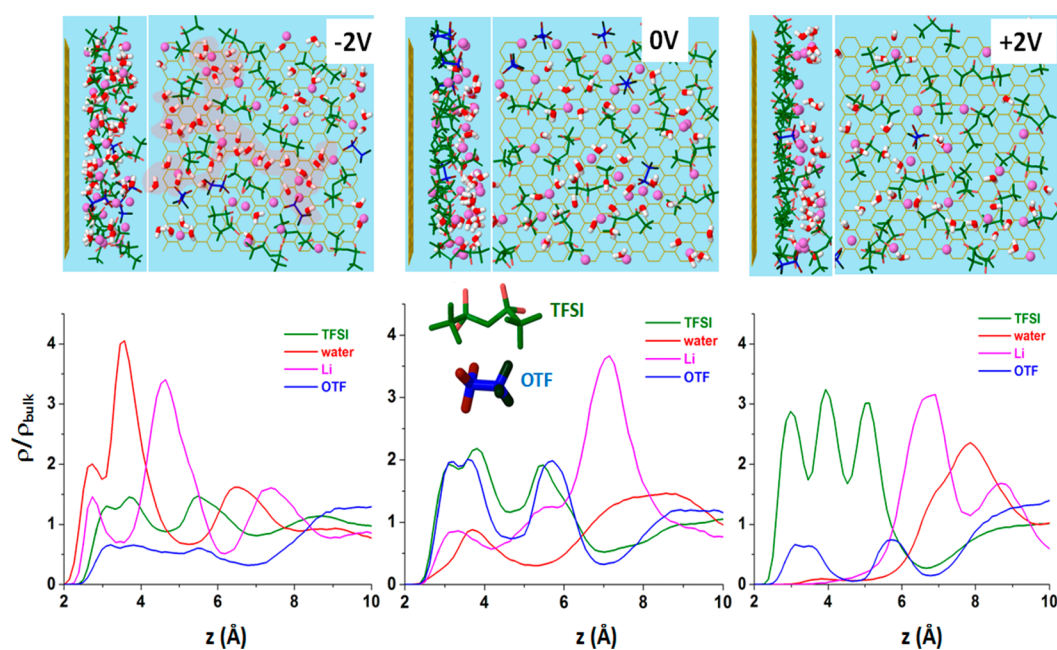


Figure 8. Cumulative atom number density profiles normalized by bulk density as a function of distance from electrode (z), snapshots of the interfacial layer at -2 , 0 , and 2 V vs PZC. Reproduced with permission from ref 55. Copyright 2017 American Chemical Society.

among the $\text{Li}^+(\text{DMC})_4$ solvates the preference for DMCcc versus DMCct conformer is much less. Thus, in the EC-rich electrolytes, higher reduction potentials of EC (0.6 V vs Li/Li^+) and DMCcc (0.4 V vs Li/Li^+) together with EC higher population in the Li^+ solvation are responsible for the EC dominance in SEI chemistry. Interestingly, in a single-solvent DMC-based electrolyte, the DMCcc and DMCct contributions to the Li^+ solvation shell are comparable and the electrolyte reduction is determined by the DMCct that has reduction potential of 0.6 V. Significant DMCct presence in the Li^+ solvation shell in DMC– LiPF_6 was reported from Raman measurements.⁴³

RAMIFICATIONS OF INTERFACIAL STRUCTURE TO ELECTROLYTE ELECTROCHEMICAL STABILITY

Most of our knowledge of the Li^+ solvation shell composition comes from bulk electrolytes studies while the interfacial

structure is most relevant to electrochemistry. MD simulations are used to explore this topic. The double layer structure of the mixed solvent EC/DMC(3:7)– 1 M LiPF_6 electrolyte on graphite is shown in Figure 6. At the point of zero charge (PZC), the double layer composition closely resembles bulk. Upon charging of the electrodes, the less-polar DMC molecule is partially displaced in the interfacial layer by the more-polar EC.⁴⁴ Subsequent experiments confirmed this prediction reporting a strong preferential adsorption of EC molecules on the LiCoO_2 surfaces compared to linear carbonates.⁴⁵ Interestingly, as the Li^+ with its solvation shell approaches the negative electrode surface or SEI, it tends to preferentially dissociate DMC and keep EC in its first solvation shell.^{44,46} This is an additional factor contributing to the preference of EC reduction versus DMC and dominance of EC reduction products in SEI formed from the EC/DMC mixed electrolytes. At the positive

electrode, PF_6^- rapidly accumulates at the electrode surface with increasing potential and is likely to participate in oxidation (see Figure 2). Ionic liquids showed a complete separation of co- and counterions at highly charged electrodes at $\sim 4\text{--}5\text{ V}$ with the counterions adsorbed at the electrode surface and the co-ion excluded from direct interaction with the electrode.⁴⁷ Experimental observation of higher resistance against oxidation for the highly concentrated carbonate electrolyte with LiTFSI provided an experimental support to this hypothesis.⁴⁸ The adsorption of TFSI⁻ anion and solvent exclusion from direct contact with the positively charged Al current collector was suggested.⁴⁸ We performed MD simulations of LiTFSI(DMC)_{1,2} electrolyte that confirmed that DMC is largely excluded from direct contact with positive electrode, as shown in Figure 7. In contrast, only about 30% of the inner Helmholtz layer was occupied by anions at low salt concentrations (see Figure 6) making solvent accessible for oxidation reactions.

Similar interfacial structure was observed for the newly discovered water-in-salt electrolytes (WiSE) that has resulted resulting a paradigm shift in aqueous electrochemistry with a significantly expanded stability window,^{32,49–51} MD simulations of WiSE comprising 21 mol/kg (molal, *m*) of LiTFSI and 7 *m* of LiOTF were performed.^{33,52} The EDL structure in WiSE was examined by analyzing the density profiles normalized by a bulk concentration of ions and water as shown in Figure 8. At PZC, the TFSI⁻ and OTF⁻ anions have the highest peaks near the electrode surface, indicating anion enrichment at the interface compared to bulk electrolytes. The $\text{Li}^+\cdots\text{F}$ contacts were found resulting in LiF formation after reduction (see Figure 4a). PZC is considered to be similar to the open circuit voltage, which is around 3 V vs Li/Li⁺ for this system. At PZC, water has a small peak around 3.8 Å from the interface. Water is partially excluded from direct interaction with the electrodes minimizing its reduction.

At the negative electrode at -2 V vs PZC (1 V vs Li/Li⁺), the water peak increases dramatically, exceeding the magnitude of TFSI⁻ peak. Water adsorbs onto the electrode surface with the hydrogen bond in a configuration preferable for H₂ evolution. The Li⁺ are also attracted to the negative electrode, as expected, but clearly not to the same extent as water because many of Li⁺ are hydrated by multiple waters. To circumvent the undesired preferential adsorption thus incurred, alternative means had to be adopted to physically expel water molecules from anode surfaces, so that “cathodic challenge” could be resolved and a $>4.0\text{ V}$ stability window could be realized with aqueous electrolyte.⁵³

Increasing the EDL potential from PZC to $+2\text{ V}$ ($\sim 5\text{ V}$ vs Li/Li⁺) significantly increases the TFSI⁻ anion adsorption at the interface, while pushing water and OTF⁻ anions away from direct contact with the electrode. This mechanism is responsible for further extension of WiSE electrochemical stability window in addition to the previously suggested one due to decreased free water fraction³³ and shifts in the anion and water density of states with increasing salt concentration.³² In the situation when only TFSI⁻ is in direct contact with the electrode surface, its oxidation stability is one of the primary factors determining electrolyte oxidation stability. Because most of the TFSI⁻ anions are coordinated by Li⁺, their oxidation potential is increased by $\sim 0.3\text{ V}$ at high concentration as compared to TFSI⁻ not coordinating Li⁺, as shown in Figure S12 in McOwen et al.⁴⁸ Even higher solvent stabilization due to Li⁺ binding was claimed for glyme–LiTFSI solvates.⁵⁴ As the electrode becomes positively charged, the O(TFSI) atoms have the highest affinity to the surface. Surprisingly, there is a depletion of O(OTF)

within 5 Å of the surface at 2 V, indicating that O(OTF) desorbs as the electrode becomes more positive. This opposite behavior of O(OTF) versus O(TFSI) seems to contradict the expectation of a stronger adsorption of O(OTF) versus O(TFSI) due to its higher negative partial charge on oxygens, which should screen a positive electrode charge more effectively. This apparent paradox is resolved by examining the double layer structure. Unlike TFSI⁻, which adsorbs parallel to the surface and coordinates both the positive surface and Li⁺ cations in the second interfacial layer, OTF⁻ coordinates the Li⁺ located in the second interfacial layer leaving its CF₃⁻ oriented toward the positive electrode. It leads to less favorable electrode charge screening by OTF⁻ versus TFSI⁻.⁵⁵

This intriguing phenomena in light of recent sacrificial anion additive development⁵⁶ was investigated by difference electrochemical internal attenuated total reflection FTIR measurement method on Pt electrode as discussed in detail in SI. The high surface roughness of the thin electrode enhances the detection limit through the surface enhancement IR adsorption (SEIRA) effects. Changes in adsorption with applied potentials relative to the reference potential in the frequency range that exhibits strong adsorption bands at 1183–1194 and 1280–1302 cm⁻¹ for OTF⁻ and 1225 and 1245 cm⁻¹ TFSI⁻ bands as shown Figure 9. These measurements confirm MD prediction of the

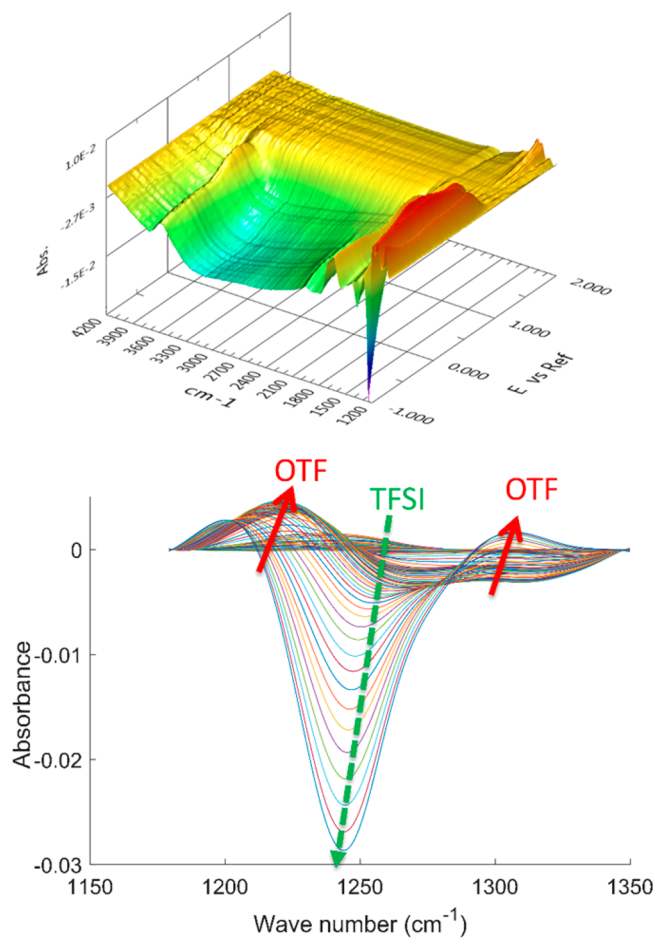


Figure 9. DEC-IATR-FTIR spectra of 21m LiTFSI + 7m LiOTF electrolyte on Pt at room temperature as a function of electrode potential relative to a reference spectrum at 1.4 V vs Ag/AgCF₃SO₃. Bottom figure shows the directions of TFSI⁻ and OTF⁻ peak intensities as the electrode potential decreases from 2.2 V to -0.5 V vs Ag/AgCF₃SO₃.

preferential adsorption of TFSI⁻ and exclusion of OTF⁻ from the electrode with increasing potential.

SUMMARY

A combination of QC calculations and MD simulations of electrolyte structure in bulk and at interfaces provided important insight into control mechanisms for manipulating electrolyte oxidation and reduction stability and interphasial chemistries. Excluding certain solvent and anions from direct interaction with electrode surfaces gives a possibility to tailor an interphasial structure. The solvent exclusion mechanism for extending electrolyte oxidation stability does not rely on passivation layer formation and, therefore, could potentially be used for extending the EDL capacitor window range without clogging pores and losing electrolyte. Anion and solvent defluorination reactions coupled with reduction are more energetically favorable than solvent reduction without defluorination but are kinetically slower due to larger reorganization energy. Analogously, H-transfer coupled with solvent oxidation occurs for carbonate, phosphate, and sulfone solvents.

ASSOCIATED CONTENT

Supporting Information

The Supporting Information is available free of charge on the ACS Publications website at DOI: 10.1021/acs.accounts.7b00486.

Description of MD simulations and spectroscopy measurements (PDF)

AUTHOR INFORMATION

Corresponding Author

*E-mail: oleg.a.borodin.civ@mail.mil.

ORCID

Oleg Borodin: 0000-0002-9428-5291

Notes

The authors declare no competing financial interest.

Biographies

Oleg Borodin, Ph.D. (University of Utah, 2000), works on modeling of battery electrolytes and electrochemical interfaces.

Xiaoming Ren, Ph.D. (1993), works on in situ surface-enhanced infrared spectroscopy to study electrochemical processes.

Jenel Vatamanu, Ph.D. (Queen's University, Canada), focuses on modeling of electrified interfaces.

Arthur von Wald Cresce, Ph.D. (University of Maryland – College Park), has research interest in fundamental characterization and development of battery materials.

Jaroslav Knap, Ph.D. (Arizona State University, 1998), team leader, works on development of computational methods for materials.

Kang Xu, Ph.D. in Chemistry (Arizona State University, 1995), is a Lab Fellow and team leader with research interest in electrolyte materials and fundamental science of interphasial processes.

REFERENCES

(1) Xu, K. Electrolytes and Interphases in Li-Ion Batteries and Beyond. *Chem. Rev.* **2014**, *114*, 11503–11618.
(2) Ue, M.; Sasaki, Y.; Tanaka, Y.; Morita, M. Nonaqueous Electrolytes with Advances in Solvents. In *Electrolytes for Lithium and Lithium-Ion Batteries*; Jow, T. R., Xu, K., Borodin, O., Ue, M., Eds.; Springer: New York, 2014; Vol. 58, pp 93–165.

(3) Leung, K. Two-Electron Reduction of Ethylene Carbonate: A Quantum Chemistry Re-Examination of Mechanisms. *Chem. Phys. Lett.* **2013**, *568*, 1–8.

(4) Xu, K. Nonaqueous Liquid Electrolytes for Lithium-Based Rechargeable Batteries. *Chem. Rev.* **2004**, *104*, 4303–4417.

(5) Xu, M.; Xing, L.; Li, W. Interphases between Electrolytes and Anodes in Li-Ion Battery. In *Electrolytes for Lithium and Lithium-Ion Batteries*; Jow, T. R., Xu, K., Borodin, O., Ue, M., Eds.; Springer: New York, 2014; Vol. 58, pp 227–282.

(6) Sodeyama, K.; Yamada, Y.; Aikawa, K.; Yamada, A.; Tateyama, Y. Sacrificial Anion Reduction Mechanism for Electrochemical Stability Improvement in Highly Concentrated Li-Salt Electrolyte. *J. Phys. Chem. C* **2014**, *118*, 14091–14097.

(7) Kim, H.; Wu, F.; Lee, J. T.; Nitta, N.; Lin, H.-T.; Oschatz, M.; Cho, W. I.; Kaskel, S.; Borodin, O.; Yushin, G. In Situ Formation of Protective Coatings on Sulfur Cathodes in Lithium Batteries with Lifsi-Based Organic Electrolytes. *Adv. Energy Mater.* **2015**, *5*, 1401792.

(8) Borodin, O.; Behl, W.; Jow, T. R. Oxidative Stability and Initial Decomposition Reactions of Carbonate, Sulfone, and Alkyl Phosphate-Based Electrolytes. *J. Phys. Chem. C* **2013**, *117*, 8661–8682.

(9) Borodin, O. Molecular Modeling of Electrolytes. In *Electrolytes for Lithium and Lithium-Ion Batteries*; Jow, T. R., Xu, K., Borodin, O., Ue, M., Eds.; Springer: New York, 2014; Vol. 58, pp 371–401.

(10) Borodin, O.; Olguin, M.; Spear, C. E.; Leiter, K.; Knap, J. Towards High Throughput Screening of Electrochemical Stability of Battery Electrolytes. *Nanotechnology* **2015**, *26*, 354003.

(11) Wang, R. L.; Buhmester, C.; Dahn, J. R. Calculations of Oxidation Potentials of Redox Shuttle Additives for Li-Ion Cells. *J. Electrochem. Soc.* **2006**, *153*, A445–A449.

(12) Fu, Y.; Liu, L.; Yu, H. Z.; Wang, Y. M.; Guo, Q. X. Quantum-Chemical Predictions of Absolute Standard Redox Potentials of Diverse Organic Molecules and Free Radicals in Acetonitrile. *J. Am. Chem. Soc.* **2005**, *127*, 7227–7234.

(13) Johansson, P. Intrinsic Anion Oxidation Potentials. *J. Phys. Chem. A* **2007**, *111*, 1378–1379.

(14) Yoshitake, H. Functional Electrolytes Specially Designed for Lithium Batteries. In *Lithium-Ion Batteries*; Yoshio, M., Ed.; Springer Science + Business Media LLC: 2009; pp 343–366.

(15) Shkrob, I. A.; Zhu, Y.; Marin, T. W.; Abraham, D. Reduction of Carbonate Electrolytes and the Formation of Solid-Electrolyte Interface (SEI) in Lithium-Ion Batteries. 1. Spectroscopic Observations of Radical Intermediates Generated in One-Electron Reduction of Carbonates. *J. Phys. Chem. C* **2013**, *117*, 19255–19269.

(16) Delp, S. A.; Borodin, O.; Olguin, M.; Eisner, C. G.; Allen, J. L.; Jow, T. R. Importance of Reduction and Oxidation Stability of High Voltage Electrolytes and Additives. *Electrochim. Acta* **2016**, *209*, 498–510.

(17) Ue, M.; Murakami, A.; Nakamura, S. Anodic Stability of Several Anions Examined by Ab Initio Molecular Orbital and Density Functional Theories. *J. Electrochem. Soc.* **2002**, *149*, A1572–A1577.

(18) Kumar, N.; Leung, K.; Siegel, D. J. Crystal Surface and State of Charge Dependencies of Electrolyte Decomposition on LiMn₂O₄ Cathode. *J. Electrochem. Soc.* **2014**, *161*, E3059–E3065.

(19) Giordano, L.; Karayaylali, P.; Yu, Y.; Katayama, Y.; Maglia, F.; Lux, S.; Shao-Horn, Y. Chemical Reactivity Descriptor for the Oxide-Electrolyte Interface in Li-Ion Batteries. *J. Phys. Chem. Lett.* **2017**, *8*, 3881–3887.

(20) Shkrob, I. A.; Abraham, D. P. Electrocatalysis Paradigm for Protection of Cathode Materials in High-Voltage Lithium-Ion Batteries. *J. Phys. Chem. C* **2016**, *120*, 15119–15128.

(21) Leung, K. First-Principles Modeling of Mn(II) Migration above and Dissolution from Li_xMn₂O₄ (001) Surfaces. *Chem. Mater.* **2017**, *29*, 2550–2562.

(22) Burkhardt, S. E. Impact of Chemical Follow-up Reactions for Lithium Ion Electrolytes: Generation of Nucleophilic Species, Solid Electrolyte Interphase, and Gas Formation. *J. Electrochem. Soc.* **2017**, *164*, A684–A690.

- (23) Leung, K.; Tenney, C. M. Toward First Principles Prediction of Voltage Dependences of Electrolyte/Electrolyte Interfacial Processes in Lithium Ion Batteries. *J. Phys. Chem. C* **2013**, *117*, 24224–24235.
- (24) Leung, K.; Soto, F.; Hankins, K.; Balbuena, P. B.; Harrison, K. L. Stability of Solid Electrolyte Interphase Components on Lithium Metal and Reactive Anode Material Surfaces. *J. Phys. Chem. C* **2016**, *120*, 6302–6313.
- (25) Li, Y.; Leung, K.; Qi, Y. Computational Exploration of the Li-Electrode/Electrolyte Interface in the Presence of a Nanometer Thick Solid-Electrolyte Interphase Layer. *Acc. Chem. Res.* **2016**, *49*, 2363–2370.
- (26) Leung, K.; Rempe, S. B.; Foster, M. E.; Ma, Y.; Martinez del la Hoz, J. M.; Sai, N.; Balbuena, P. B. Modeling Electrochemical Decomposition of Fluoroethylene Carbonate on Silicon Anode Surfaces in Lithium Ion Batteries. *J. Electrochem. Soc.* **2014**, *161*, A213–A221.
- (27) Wang, Z.-C.; Xu, J.; Yao, W.-H.; Yao, Y.-W.; Yang, Y. Fluoroethylene Carbonate as an Electrolyte Additive for Improving the Performance of Mesocarbon Microbead Electrode. *ECS Trans.* **2011**, *41*, 29–40.
- (28) Yang, Z.; Gewirth, A. A.; Trahey, L. Investigation of Fluoroethylene Carbonate Effects on Tin-Based Lithium-Ion Battery Electrodes. *ACS Appl. Mater. Interfaces* **2015**, *7*, 6557–6566.
- (29) Zhang, Z.; Hu, L.; Wu, H.; Weng, W.; Koh, M.; Redfern, P. C.; Curtiss, L. A.; Amine, K. Fluorinated Electrolytes for 5 V Lithium-Ion Battery Chemistry. *Energy Environ. Sci.* **2013**, *6*, 1806–1810.
- (30) von Wald Cresce, A.; Borodin, O.; Xu, K. Correlating Li⁺ Solvation Sheath Structure with Interphasial Chemistry on Graphite. *J. Phys. Chem. C* **2012**, *116*, 26111–26117.
- (31) Borodin, O.; Suo, L.; Gobet, M.; Ren, X.; Wang, F.; Faraone, A.; Peng, J.; Olguin, M.; Schroeder, M.; Ding, M. S.; Gobrogge, E.; von Wald Cresce, A.; Munoz, S.; Dura, J. A.; Greenbaum, S.; Wang, C.; Xu, K. Liquid Structure with Nano-Heterogeneity Promotes Cationic Transport in Concentrated Electrolytes. *ACS Nano* **2017**, *11*, 10462–10471.
- (32) Suo, L.; Borodin, O.; Gao, T.; Olguin, M.; Ho, J.; Fan, X.; Luo, C.; Wang, C.; Xu, K. Water-in-Salt[™] Electrolyte Enables High-Voltage Aqueous Lithium-Ion Chemistries. *Science* **2015**, *350*, 938–943.
- (33) Suo, L.; Borodin, O.; Sun, W.; Fan, X.; Yang, C.; Wang, F.; Gao, T.; Ma, Z.; Schroeder, M.; von Cresce, A.; Russell, S. M.; Armand, M.; Angell, A.; Xu, K.; Wang, C. Advanced High-Voltage Aqueous Lithium-Ion Battery Enabled by “Water-in-Bisalt” Electrolyte. *Angew. Chem., Int. Ed.* **2016**, *55*, 7136–7141.
- (34) Suo, L.; Borodin, O.; Wang, Y.; Rong, X.; Sun, W.; Fan, X.; Xu, S.; Schroeder, M. A.; Cresce, A. V.; Wang, F.; Yang, C.; Hu, Y.-S.; Xu, K.; Wang, C. Water-in-Salt[™] Electrolyte Makes Aqueous Sodium-Ion Battery Safe, Green, and Long-Lasting. *Adv. Energy Mater.* **2017**, *7*, 1701189.
- (35) Xu, K.; Lam, Y. F.; Zhang, S. S.; Jow, T. R.; Curtis, T. B. Solvation Sheath of Li⁺ in Nonaqueous Electrolytes and Its Implication of Graphite/Electrolyte Interface Chemistry. *J. Phys. Chem. C* **2007**, *111*, 7411–7421.
- (36) von Cresce, A.; Xu, K. Preferential Solvation of Li⁺ Directs Formation of Interphase on Graphitic Anode. *Electrochem. Solid-State Lett.* **2011**, *14*, A154–A156.
- (37) Xu, K.; von Cresce, A. Interfacing Electrolytes with Electrodes in Li Ion Batteries. *J. Mater. Chem.* **2011**, *21*, 9849–9864.
- (38) Morita, M.; Asai, Y.; Yoshimoto, N.; Ishikawa, M. A Raman Spectroscopic Study of Organic Electrolyte Solutions Based on Binary Solvent Systems of Ethylene Carbonate with Low Viscosity Solvents Which Dissolve Different Lithium Salts. *J. Chem. Soc., Faraday Trans.* **1998**, *94*, 3451–3456.
- (39) Seo, D. M.; Reiningger, S.; Kutcher, M.; Redmond, K.; Euler, W. B.; Lucht, B. L. Role of Mixed Solvation and Ion Pairing in the Solution Structure of Lithium Ion Battery Electrolytes. *J. Phys. Chem. C* **2015**, *119*, 14038–14046.
- (40) Yang, L.; Xiao, A.; Lucht, B. L. Investigation of Solvation in Lithium Ion Battery Electrolytes by Nmr Spectroscopy. *J. Mol. Liq.* **2010**, *154*, 131–133.
- (41) Bogle, X.; Vazquez, R.; Greenbaum, S.; Cresce, A. v. W.; Xu, K. Understanding Li⁺-Solvent Interaction in Nonaqueous Carbonate Electrolytes with ¹⁷O Nmr. *J. Phys. Chem. Lett.* **2013**, *4*, 1664–1668.
- (42) Borodin, O.; Olguin, M.; Ganesh, P.; Kent, P. R. C.; Allen, J. L.; Henderson, W. A. Competitive Lithium Solvation of Linear and Cyclic Carbonates from Quantum Chemistry. *Phys. Chem. Chem. Phys.* **2016**, *18*, 164–175.
- (43) Chapman, N.; Borodin, O.; Yoon, T.; Nguyen, C. C.; Lucht, B. L. Spectroscopic and Density Functional Theory Characterization of Common Lithium Salt Solvates in Carbonate Electrolytes for Lithium Batteries. *J. Phys. Chem. C* **2017**, *121*, 2135–2148.
- (44) Vatamanu, J.; Borodin, O.; Smith, G. D. Molecular Dynamics Simulation Studies of the Structure of a Mixed Carbonate/LiPF₆ Electrolyte near Graphite Surface as a Function of Electrode Potential. *J. Phys. Chem. C* **2012**, *116*, 1114–1121.
- (45) Yu, L.; Liu, H.; Wang, Y.; Kuwata, N.; Osawa, M.; Kawamura, J.; Ye, S. Preferential Adsorption of Solvents on the Cathode Surface of Lithium Ion Batteries. *Angew. Chem.* **2013**, *125*, 5865–5868.
- (46) Borodin, O.; Bedrov, D. Interfacial Structure and Dynamics of the Lithium Alkyl Dicarboxylate SEI Components in Contact with the Lithium Battery Electrolyte. *J. Phys. Chem. C* **2014**, *118*, 18362–18371.
- (47) Vatamanu, J.; Borodin, O.; Smith, G. D. Molecular Insights into the Potential and Temperature Dependences of the Differential Capacitance of a Room-Temperature Ionic Liquid at Graphite Electrodes. *J. Am. Chem. Soc.* **2010**, *132*, 14825–14833.
- (48) McOwen, D. W.; Seo, D. M.; Borodin, O.; Vatamanu, J.; Boyle, P. D.; Henderson, W. A. Concentrated Electrolytes: Decrypting Electrolyte Properties and Reassessing Al Corrosion Mechanisms. *Energy Environ. Sci.* **2014**, *7*, 416–426.
- (49) Yamada, Y.; Usui, K.; Sodeyama, K.; Ko, S.; Tateyama, Y.; Yamada, A. Hydrate-Melt Electrolytes for High-Energy-Density Aqueous Batteries. *Nature Energy* **2016**, *1*, 16129.
- (50) Suo, L.; Han, F.; Fan, X.; Liu, H.; Xu, K.; Wang, C. “Water-in-Salt” Electrolytes Enable Green and Safe Li-Ion Batteries for Large Scale Electric Energy Storage Applications. *J. Mater. Chem. A* **2016**, *4*, 6639–6644.
- (51) Ramanujapuram, A.; Gordon, D.; Magasinski, A.; Ward, B.; Nitta, N.; Huang, C.; Yushin, G. Degradation and Stabilization of Lithium Cobalt Oxide in Aqueous Electrolytes. *Energy Environ. Sci.* **2016**, *9*, 1841.
- (52) Yang, C.; Suo, L.; Borodin, O.; Wang, F.; Sun, W.; Gao, T.; Fan, X.; Hou, S.; Ma, Z.; Amine, K.; Xu, K.; Wang, C. Unique Aqueous Li-Ion/Sulfur Chemistry with High Energy Density and Reversibility. *Proc. Natl. Acad. Sci. U. S. A.* **2017**, *114*, 6197–6202.
- (53) Yang, C.; Chen, J.; Qing, T.; Fan, X.; Sun, W.; von Cresce, A.; Ding, M. S.; Borodin, O.; Vatamanu, J.; Schroeder, M. A.; Eidson, N.; Wang, C.; Xu, K. 4.0 V Aqueous Li-Ion Batteries. *Joule* **2017**, *1*, 122–132.
- (54) Yoshida, K.; Nakamura, M.; Kazue, Y.; Tachikawa, N.; Tsuzuki, S.; Seki, S.; Dokko, K.; Watanabe, M. Oxidative-Stability Enhancement and Charge Transport Mechanism in Glyme-Lithium Salt Equimolar Complexes. *J. Am. Chem. Soc.* **2011**, *133*, 13121–13129.
- (55) Vatamanu, J.; Borodin, O. Ramifications of Water-in-Salt Interfacial Structure at Charged Electrodes for Electrolyte Electrochemical Stability. *J. Phys. Chem. Lett.* **2017**, *8*, 4362–4367.
- (56) Xu, M.; Zhou, L.; Dong, Y.; Chen, Y.; Demeaux, J.; MacIntosh, A. D.; Garsuch, A.; Lucht, B. L. Development of Novel Lithium Borate Additives for Designed Surface Modification of High Voltage LiNi_{0.5}Mn_{1.5}O₄ Cathodes. *Energy Environ. Sci.* **2016**, *9*, 1308–1319.
- (57) Wu, F.; Borodin, O.; Yushin, G. In Situ Surface Protection for Enhancing Stability and Performance of Conversion-Type Cathodes. *MRS Energy & Sustainability* **2017**, *4*, e9.
- (58) Borodin, O.; Olguin, M.; Spear, C.; Leiter, K.; Knap, J.; Yushin, G.; Childs, A.; Xu, K. Challenges with Quantum Chemistry-Based Screening of Electrochemical Stability of Lithium Battery Electrolytes. *ECS Trans.* **2015**, *69*, 113–123.